World Academy of Science, Engineering and Technology
International Journal of Materials and Metallurgical Engineering
Vol:5, No:7, 2011

Structural and Electronic Characterization of Supported Ni and Au Catalysts used in Environment Protection Determined by XRD, XAS and XPS methods

N. Aldea, V. Rednic, F. Matei, Tiandou Hu and M. Neumann

***Abstract*—**The nickel and gold nanoclusters as supported catalysts were analyzed by XAS, XRD and XPS in order to determine their local, global and electronic structure. The present study has pointed out a strong deformation of the local structure of the metal, due to its interaction with oxide supports. The average particle size, the mean squares of the microstrain, the particle size distribution and microstrain functions of the supported Ni and Au catalysts were determined by XRD method using Generalized Fermi Function for the X-ray line profiles approximation. Based on EXAFS analysis we consider that the local structure of the investigated systems is strongly distorted concerning the atomic number pairs. Metal-support interaction is confirmed by the shape changes of the probability densities of electron transitions: Ni K edge (1s $\rightarrow$ continuum and 2p), Au L_{III}-edge ($2p_{3/2} \rightarrow$ continuum, 6s, $6d_{5/2}$ and $6d_{3/2}$). XPS investigations confirm the metal-support interaction at their interface.

***Keywords*—**local and global structure, metal-support interaction, supported metal catalysts, synchrotron radiation, X-ray absorption spectroscopy, X-ray diffraction, X-ray photoelectron spectroscopy.

I. Introduction

ELECTRONIC and structural information about the local vicinity around a specific atomic constituent in the amorphous materials [1, 2], the location and chemical state of any catalytic atom on different oxide supports [3] and nanoparticle of transition metal oxides [4-6] can be obtained through X-ray absorption spectroscopy (XAS) technique.

X-ray absorption near edge structure (XANES) is sensitive to local geometries and electronic structure of atoms that constitute the nanoparticles. The changes of the coordination geometry and the oxidation state upon decreasing the crystallite size and the interaction with supports on metal nanoparticles surface can be extracted from XANES spectrum.

Extended X-ray absorption fine structure (EXAFS) is a specific element of the scattering technique in which a core electron ejected by an X-ray photon probes the local environment of the absorbing atom. The ejected photoelectron backscattered by the neighbouring atoms around the absorbing atom interferes constructively with the outgoing electron wave, depending on the energy of the photoelectron.

X-ray diffraction (XRD) line broadening investigations of nanostructured materials is limited to find the average crystallite size from the integral breadth or the full width at half maximum (FWHM) of a diffraction profile. In the case of nanostructured materials due to the difficulty of performing satisfactory intensity measurements on the higher order reflections, it is impossible to obtain two orders of (*hkl*) profile. Consequently, it is not possible to apply the classical method of Warren and Averbach [7] or the subsequent developed method of Balzar at al., based on Voigt approximation [8]. In this paper we developed a rigorous analysis of the X-ray line profile (XRLP) in terms of Fourier transform where zero strains assumption is not required. The apparatus employed in a measurement generally affects the obtained data and a considerable amount of work has been done to make resolution corrections. In the case of XRLP, the convolution of true data function by the instrumental function produced by a well-annealed sample is described by Fredholm integral equation of the first kind [9]. A rigorous way for solving this equation is Stokes method based on Fourier transform technique. The X-Ray photoelectron spectroscopy (XPS) technique was used for determining the electronic states of gold and nickel together with their metal oxides supports. The following catalyst samples were investigated: Ni/Cr_2O_3 treated at 420 and 650 °C temperatures, $Au/MnO_x/Al_2O_3$ and Au/Al_2O_3. The Ni/Cr_2O_3 catalysts are applied for H/D reaction between hydrogen and water vapour [10]. The supported gold catalysts are used in redaction or oxidation of NO applied in the environment protection [11, 12].

N. A. Author is with the National Institute for Research and Development of Isotopic and Molecular Technologies, Cluj-Napoca, 400293, Romania (phone: +40264-584.037; fax: +40264-420.042; e-mail: naldea@itim-cj.ro).

V. R. Author is with the National Institute for Research and Development of Isotopic and Molecular Technologies, Cluj-Napoca, 400293, Romania (e-mail: vrednic@itim-cj.ro).

F. M. Author is with the Agriculture Sciences and Medicine Veterinary University, Department of Mathematical and Computer Science, Cluj-Napoca, Romania, (e-mail: faldea@usamvcluj.ro).

T. H. Author is with Beijing Synchrotron Radiation Facilities of Beijing Electron Positron Collider National Laboratory, People's Republic of China (e-mail: hutd@ihep.ac.cn).

M. N. Author is with the University of Osnabrück, Fachberiech Physik, 49069 Osnabrück, Germany (e-mail: mneumann@uos.de).

II. Experimental and Data Processing

A. Samples preparation

The Ni/Cr_2O_3 systems treated at 420 and 650 °C temperatures were prepared by coprecipitation method [13]. The precursor materials used for preparation of the supported gold catalysts were $HAuCl_4$ $3H_2O$, urea $(NH_2)2CO$ p.a. and γ - Al_2O_3. Atomic ratio Au:Al was 1:75. The nanosized Au/Al_2O_3 was prepared by homogeneous deposition-precipitation (HDP) using excess urea as precipitating agent [14]. The $Au/MnO_x/Al_2O_3$ has been prepared by impregnation under vacuum conditions where atomic ratio Mn:Al was 1:15 [15].

B. Measurement methods

The transmission and fluorescence EXAFS measurements on Ni K and Au L_{III} edges were carried out on *4W1B* beamline in Beijing Synchrotron Radiation Facilities operating at 30-50 mA and 2.2 GeV [16]. The beamline *4W1B* is an unfocussed monochromatic X-ray beam with 4 mrad of horizontal acceptance. The X-rays are monochromatized by a fixed exit *Si* double crystal monochromator. The features of *4W1B* beamline are: energy range of *3.5-22 KeV*, energy resolution of ΔE*=0.5-2 eV* at E *=10KeV*, Bragg angle range of *5-70*^{0}, the crystals Si(111), Si(220) and Si(311) can be alternatively used. A Ni and Au foils were used as a standard samples. The absorption coefficients of Ni K and Au L_{III} edges were determined using a Si (111) double-crystal monochromator. The absorption coefficients were measured in an energy scale from 8186 to 9331 eV for Ni and 11500 to 12808 eV for Au, respectively. Harmonics were rejected by detuning of the monochromator. Special care was taken in preparation of the samples for measurements, especially for thickness and homogeneity of samples to obtain absorption spectra of good quality. All samples were ground to fine powder and homogeneously dusted on scotch tape. The EXAFS analysis of the absorption coefficient was processed by computer codes EXAFS51 to EXAFS56 [17] from our library.

The XRD measurements for supported nickel catalysts were realized on beamline *4W1C* that is a time-shared branch with beamline *4W1B*. The energy resolution is *0.5 eV* at *0.154 nm*. A *NaI(Tl)* detector was used, signals were amplified and fed to a single channel analyser *(ORTEC 850)* and read out by a computer. A silicon powder was used as standard sample for instrumental correction. The XRD measurements range, 2θ, was from *28*^{0} to *70*^{0}. The X-ray diffraction data for supported gold catalysts were collected using a Rigaku rotating anode setup in Bragg-Brentano geometry with Ni filtered Cu K_α radiation, λ=1.5406 Å at room temperature. The Fourier transform of the supported nickel and gold catalysts XRLP (111), (200) and (220) as well as (111), (200), (220) and (311), respectively were processed by computer code SIZE developed with Maple software. This computer code is improved version of XRLINE [9] and XRLINE1 [18] computer programs, respectively. Its purpose is to show intermediate processing results in a graphic manner.

The XPS spectra were recorded using a PHI 5600ci ESCA spectrometer with monochromatic Al K_α X-ray radiation (1486.6 eV) at room temperature. The pressure in the ultra-high vacuum chamber was within the 10^{-10} mbar range during the measurements. A neutralizer was used in every case due to a charge effect which occurs for non-conducting samples. The binding energy was determined by reference to the C 1s line at 284.8 eV. SimPeak and Unifit computer packages programs were used for data analysis of the XPS spectra. They are globally approximated by the asymmetric Donjac-Sunjic distribution using Levenberg Marquardt algorithm. For background correction we used Shirley and Tougaard algorithm based on mathematical description of the electron transport.

III. Results and Discussion

A. XANES results

The electronic properties of supported nickel and gold catalysts are evidenced by the XANES analysis of the following electronic transitions: Ni K edge (1s → continuum and 2p), Au L_{III}-edge ($2p_{3/2}$ → continuum, 6s, $6d_{5/2}$ and $6d_{3/2}$). Fig. 1 shows XANES spectra for investigated nanostructured Ni/Cr_2O_3 sample in the range of -40 up 30 eV as well as the electron transition probability approximations.

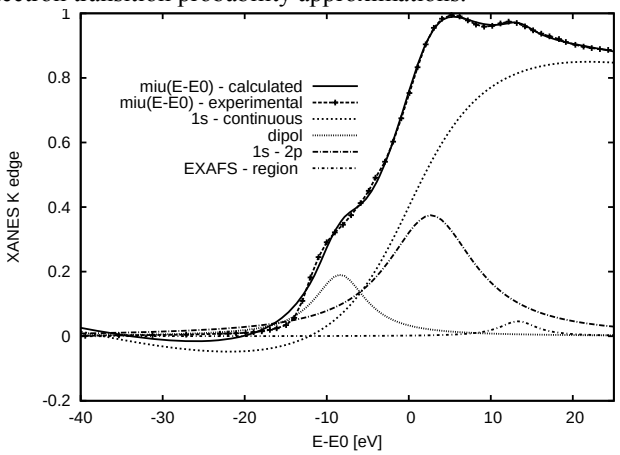

Fig. 1 The experimental and calculated XANES spectrum of Ni K edge for Ni/Cr2O3 treated at 420 ^{0}C. The last peak corresponds to the beginning of the EXAFS spectrum

The white line, which is due to a mixing process of the electrons of central metal atom with neighbouring oxygen electrons, is not present. This suggests that both Ni and Au active metals are not oxidized. Based on classical theory these electron transition probabilities have been approximated by Cauchy, and arctan distributions [19]. The main parameters are: the threshold energies, the amplitude, the position and the full width at half maximum and their values are also presented in Table I.

TABLE I
PARAMETERS OF THE ELECTRON TRANSITION PROBABILITIES(*)

Sample	Arctan distribution		Cauchy distributions					
K edge	1s → continuum		Dipole		1s → 2p		EXAFS region	
	E_0 [eV]	Γ_0 [eV]	E_1-E_0 [eV]	Γ_1 [eV]	E_2-E_0 [eV]	Γ_2 [eV]	E_3-E_0 [eV]	Γ_3 [eV]
Ni foil	8333.91	30.62	-8.39	8.72	2.68	10.91	13.17	5.24
Ni/Cr2O3 420 C	8334.06	17.23	-8.38	7.73	2.69	13.09	13.32	5.48
Ni/Cr2O3 650 C	8334.12	17.68	-8.09	8.52	2.34	11.67	13.59	6.57
L_{III} edge	$2p_{3/2}$-continuous		$2p_{3/2}$-6s		$2p_{3/2}$- $6d_{3/2}$		$2p_{3/2}$-$6d_{5/2}$	
Au foil	11918.0	5.42	2.22	18.84	26.86	7.17	49.50	21.05
Au/MnO_x/ Al_2O_3	11913.7	5.89	-1.55	13.28	27.86	17.62	52.39	20.57
Au/ Al_2O_3	11909.7	10.44	-0.32	10.32	26.26	10.95	50.21	19.37

(*) E_0 – energy binding of K and L_{III} edges, Γ_0, Γ_1, Γ_2, Γ_3 – full widths at half maximum

The parameters values are reliable because they differ with about one order of magnitude from the value of the experimental resolution. The different values of FWHM, $э_i$, compared to the standard one confirm the specific strong electronic interaction between the metal and the oxide supports. The threshold energy of XANES spectra of supported gold nanoparticles are moved to lower energy, compared to Au standard sample, with about 4 and 7*eV*. The presence of the supports Al_2O_3 and MnO_x can explain this behaviour. These features are due to strong electron interaction of gold nanocrystallites with surrounded supports. The supported Ni catalysts have also shift the threshold energy of the K edge, but the parameters of the electron transition probabilities are close to those of Ni standard. This is a measure of lower electron interaction of nickel metal nanocrystallites with chromium oxide compared to the supported gold catalysts.

B. EXAFS results

The EXAFS experimental spectra for Au/MnO_x/Al_2O_3, Au/Al_2O_3 and the gold foil are given in Fig. 2.

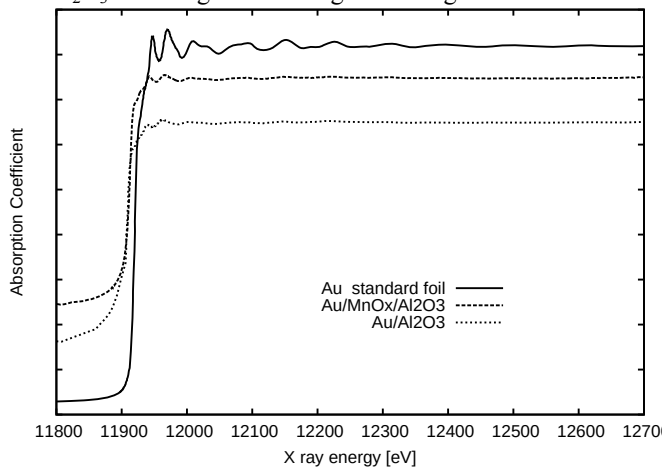

Fig. 2 The normalized absorption coefficients for the supported gold catalysts

The extraction of EXAFS signal is based on the determination of the threshold energy for Ni K and Au L_{III} edges followed by pre-edge and after-edge background removal with base line fitting using different modelling functions and by absorption coefficients evaluation with 3rd order bell spline functions [17]. The EXAFS signals of supported Ni and Au catalysts were performed in the ranges 15-160 $nm^{-1}$and 25-120 nm^{-1}, respectively. In order to obtain the distribution of the atomic distances we calculated the radial distribution function using the classical method [2, 20]. The mean Ni-Ni and Au-Au distances of the first and the second coordination shell for standard sample, at room temperature have values close to R_{Ni1}=*0.249 nm,* R_{Ni2}=*0.352 nm,* R_{Au1}=0.287 *nm* and R_{Au2}=0.407 *nm*. Based on the Fourier transform of *EXAFS* contribution, performed in the range 0.02-0.5 nm, we obtained the magnitude of the atomic radial distribution for investigated samples as well as for standard Ni and Au foils. In order to reduce the spurious errors due to limited interval in the wave vector space we have taken into consideration the Kaiser window function [17, 21]. Fig. 3 shows the Fourier transform magnitude of the investigated samples.

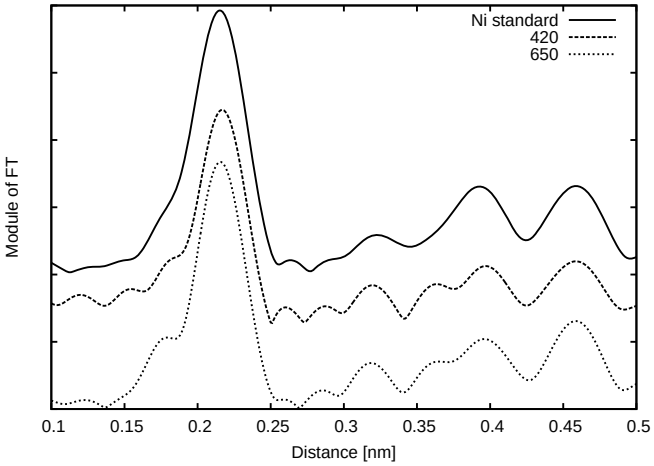

Fig. 3 The Fourier transforms of the EXAFS spectra for Ni/Cr_2O_3

The Fourier transform magnitudes are diminished as a result of the reduced average co-ordination number and their peaks are shifted from the true distance due to the phase shift function that is included in the EXAFS signal. The backscattering amplitude and the phase shift functions were obtained by analysing the Ni and Au standard samples using "small perturbation limit" method [21]. Table 2 contains the best fitting values of the local structure parameters: N, R and E_0 of the investigated samples and their uncertainties: ΔN, ΔR and ΔE_0.

TABLE II
LOCAL STRUCTURE PARAMETERS OF THE INVESTIGATED SAMPLES FOR THE FIRST COORDINATION SHELL

Sample	Coordination number $N_1 \pm \Delta N_1$	Shell radius $R_1 \pm \Delta R_1$ [nm]	Shift energy $E_0 \pm \Delta E_0$ [eV]
Ni standard	12	0.249	8333.915±0.03
Ni/Cr_2O_3 420 ^{0}C	10.18±0.09	0.2485±0.003	8334.064±0.0196
Ni/Cr_2O_3 650 ^{0}C	10.85±0.04	0.2480±0.001	8334.115±0.0503
Au standard	12	0.287	11917.04±0.04
$Au/MnO_x/Al_2O_3$	3.90±0.03	0.284±0.005	11912.22±0.02
Au/Al_2O_3	4.98±0.05	0.290±0.006	11908.31±0.03

The average interatomic distances obtained for the first coordination shell have practically the same values as those of the standard sample. Fig. 4 shows for the supported gold catalysts calculated and experimental EXAFS signal of the first shell coordination. The relative difference of the average nearest coordination number, between the standard sample and investigated catalysts, were about 16% for Ni-Ni and 58-64% for Au-Au. We have considered that these diminutions of the average nearest-neighbour coordination numbers are due to various degrees of the electron interactions between the active metal and oxide supports [22-24].

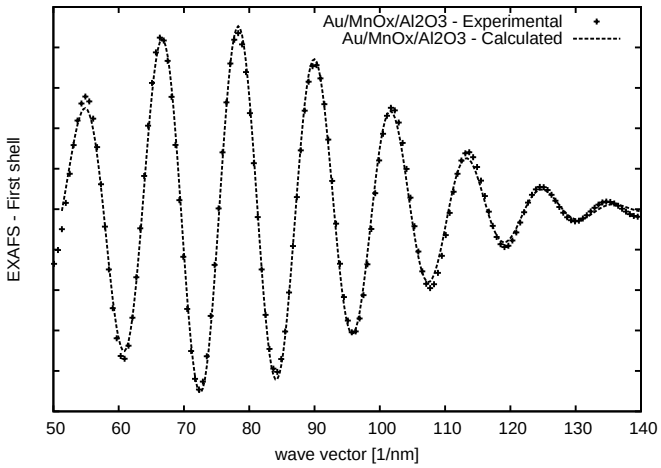

Fig. 4 The experimental and calculated EXAFS signals of the first coordination shell of $Au/MnO_x/Al_2O_3$

C. XRD results

The Fourier analysis of XRLP validity depends strongly on the magnitude and nature of the errors propagated in the data analysis. Young et al treated three systematic errors: uncorrected constant background, truncation and the effect of the sampling for the observed profile at a finite number of points that appear in discrete Fourier analysis [25]. In order to minimize propagation of these systematic errors, a global approximation of the XRLP is adopted instead of the discrete calculus. Therefore, herein the analysis of the diffraction line broadening in X-ray powder pattern was analytically calculated using the generalized Fermi function (GFF) which can have asymmetrical feature [13]. The atomic scattering factor, included in the XRLP, is asymmetric versus diffraction angle and this is why the broad peaks are best fitted by asymmetric GFF distribution. The robustness of the GFF approximation for the XRLP arises from possibility of using the analytical form of Fourier transform instead of a numerical fast Fourier transform (FFT). It is well known that validity of numerical FFT depends on the filtering technique adopted [26]. In this way validity of the microstructural parameters are closely related to accuracy of the Fourier transform magnitude of the true XRLP.

The XRLP for Ni and Au catalysts were analysed. The XRD patterns of the Ni catalysts together with standard sample used for instrumental correction are shown in Fig 5.

The next steps consist in background correction of XRLP by polynomial procedure especially in the tails domain of the profiles. The polynomial approximation is more adequate for small crystallite size determination than a constant background correction because it can avoid the "hook" effect contained in true sample function [27]. The best parameters of GFF distributions were determined by nonlinear least squares fit.

In order to determine the global nanostructure parameters of the investigated samples we computed the Fourier transforms of the true XRLP and integral width [6]. In terms of the classical Scherrer equation [28] the crystallite size is proportional with wavelength, inverse proportional with the product from cosinus of gravity centre of the true sample function and its full width at half maximum.

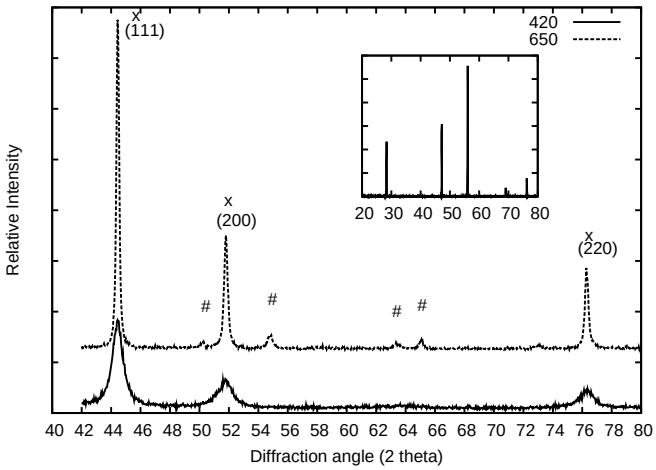

Fig. 5 The relative intensity XRLP for Ni/Cr_2O_3. x and # correspond to the Ni and oxide support contributions, respectively. Inset: the XRD spectrum for Si powder used for instrumental correction

In the Section 3.2 we have shown that the coordination shells radius of the investigated samples have similar values as the nickel and gold foils standard sample. This important result is strongly correlated with the positions of the XRLP from the experimental spectra contained in Fig. 5. Therefore, these results explain metal futures of the investigated clusters despite of strong deformation of the crystalline structure.

Hydrogen chemisorptions, transmission electron microscopy, magnetization, electronic paramagnetic resonance

and other methods could also be used to determine grain size of particles by taking into account a prior spherical form for the grains. By XRD method one can be obtain the crystallite size that has different values for the different crystallographic planes. There is a large difference between the grain size and crystallite size due to the physical meaning of the two concepts. It is possible that the grains of the active metal are built up of many metal crystallites.

The global structural parameters obtained for the investigated samples are summarized in Table 3.

TABLE III
THE GLOBAL STRUCTURE PARAMETERS OF THE INVESTIGATED SUPPORTED METAL CATALYSTS

Sample	(111)			(200)			(220)		
	D_{eff} [nm]	$<\varepsilon^2_{hkl}>$ $\times 10^4$	D_{Sch} [nm]	D_{eff} [nm]	$<\varepsilon^2_{hkl}>$ $\times 10^4$	D_{Sch} [nm]	D_{eff} [nm]	$<\varepsilon^2_{hkl}>$ $\times 10^4$	D_{Sch} [nm]
Ni85Cr15 at% 420^0C	10.5	0.2863	11.4	8.9	0.3814	8.9	8.9	0.2355	11.9
Ni85Cr15 at% 650^0C	36.4	0.0158	47.1	28.1	0.0326	30.8	30.5	0.0046	43.6
	(111)			(220)			(311)		
$Au/MnO_x/Al_2O_3$	5.2	3.6	5.6	5.2	4.1	6.01	4.3	4	4.7
Au/Al_2O_3	5.5	3.4	6	5.3	3.9	5.8	4.4	3.8	5.6

The microstrain parameter, $<\varepsilon^2_{hkl}>$, of the lattice can also be correlated with effective crystallite size, D_{eff}, in the following way: D_{eff} increases when $<\varepsilon^2_{hkl}>$ value decreases. The nanocrystallites sizes determined by Scherrer method D_{Sch} are greater than D_{eff} because Scherrer equation do not consider the lattice microstrains. Therefore, the values from Scherrer relation of Table 3 are less reliable than the results from general formula.

D.XPS results

The survey photoemission spectrum of $Au/MnO_x/Al_2O_3$ catalyst with the identification of the main XPS core level lines is presented in Fig. 6. Besides the spectral features related to the constituent elements of the supported gold catalysts only a weak C 1s peak has been detected. The presence of the C element is due to hydrocarbons absorbed on the surface of the sample powder.

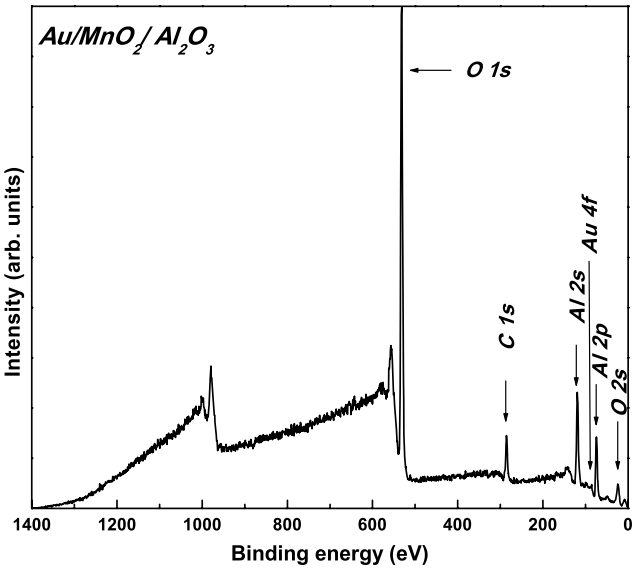

Fig. 6 XPS survey spectrum of the $Au/MnO_x/Al_20_3$ catalyst

In Fig. 7 the XPS O 1s line is presented. The two contributions from oxide supports MnO_x and Al_2O_3 can be observed.

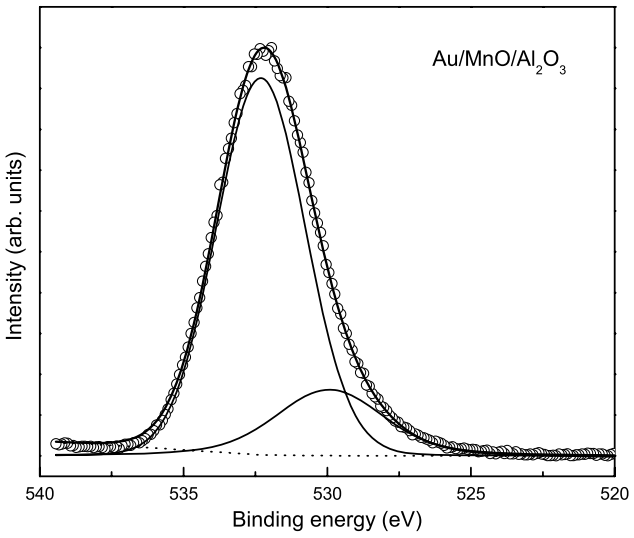

Fig. 7 XPS spectrum of O 1s lines for $Au/MnO_x/Al_20_3$ catalyst.

The Au 4f XPS spectra of the active metal, after background removal, are shown in Fig. 8.

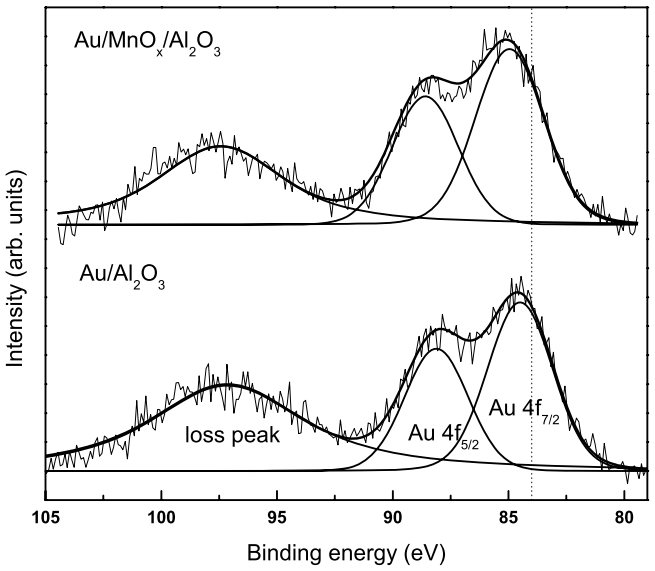

Fig. 8 XPS spectrum of Au 4f lines of investigated samples. The vertical dotted line indicates the 84 eV position

The 4f spectrum is splitted, due to the spin-orbit coupling, in two peaks corresponding to the Au $4f_{7/2}$ and Au $4f_{5/2}$ states. The binding energy of the Au $4f_{7/2}$ line is shifted to higher binding energy compared to the standard Au foil (84 eV) and has the values 84.5 and 84.9 eV for Au/Al_2O_3 and $Au/MnO_x/Al_2O_3$, respectively. This shift can be attributed to the metal-support interaction being correlated with the EXAFS results in the following way: the stronger the metal-support interaction is, local structure is more distorted concerning the diminution in the average nearest coordination number and the shift in the binding energy of the Au $4f_{7/2}$ XPS spectra is bigger. From the previous information based on EXAFS and XRD measurements such as XRLP positions and the values of the first coordination shell, we also evidenced only Au in a metal state. Along with the main lines there are loss peaks that are weaker and broader than the photoelectron peaks and appear in the spectrum at higher binding energy. Their appearance is due to the small crystallite sizes of the investigated samples.

Ni 2p spectra evidenced Ni in both metallic and oxidized states. From previous sections based on EXAFS and XRD measurements we evidenced Ni only in metallic state. The reason why EXAFS and XRD measurements cannot observe the nickel oxide is that these methods determine the crystalline structure in bulk states while XPS gives information mainly from the surface of the investigated samples. This suggests that the nickel oxide states are present only on the surface of the crystallites.

IV. Conclusion

In the present paper it has been shown how, in addition to EXAFS experiments with their specific advantages, XRD analysis can add more information for understanding nanostructure of the supported nickel and gold catalysts. Also, the XPS method provides information on the electronic structure from the surfaces of gold nanoclusters and their oxide supports. The conclusions that can be drawn from these studies are:

(i) The reduction of Au-Au and Ni-Ni coordination number from the first coordination shell of the investigated samples point out the existence of a more or less electronic interaction between the metal nanoparticles and the oxide supports.

(ii) For XRLP analysis, a global approximation is applied rather than a numerical Fourier analysis. The former analysis is better than a numerical calculation because it can minimise the systematic errors that can appear in the numerical Fourier analysis and GFF approximation of XRLP describe more accurate the broad asymmetric peaks.

(iii) Our numerical results have showed that by using the GFF distribution we have successfully obtained reliable global nanostructural parameters.

(iv) The XPS measurements confirm the presence, on the surface, of gold metallic states while Ni is in both metallic and oxidized states.

(v) The EXAFS and XPS results of Au supported catalysts are good agreement concerning the strong metal-support interaction.

Acknowledgment

The authors are grateful to BSRF for the beam time and to Dr. Xie Yaning and Dr. Zhonghua Wu for their technical assistance in EXAFS and XRD measurements. The author (N. A.) is also indebted to Professor Hu Tiandou, Director of Institute of High Energy Physics for his hospitality during the stage. This work is the result of the Scientific Cooperation Agreement between our institutes. The authors thank Dr. C. A. Gluhoi for providing the samples used in this work. This work was supported by the research programmers of Romanian Ministry of Education and Research (PN II projects nr. 22098/2008 and 32119/2008).

References

[1] E. A. Stern, "Theory of EXAFS" in *X-ray absorption: principles, applications, techniques of EXAFS, SEXAFS and XANES*, D.C. Koningsberger, R. Prins, Ed. New York: Weley, 1988.

[2] F. W Lytle, D. E. Sayers and E. A. Stern, "Report of the international workshop on standards and criteria in X-ray absorption spectroscopy", *Physica B*, vol. 158, pp. 701-722, 1989.

[3] J. H Sinfelt, G. H. Via and F. W. Lytle, "Application of EXAFS in catalysis. Structure of bimetallic cluster catalysts", *Catal. Rev. Sci. Eng.*, vol. 26, pp. 81-140, 1984

[4] L. X Chen, T. Liu, M. C. Thurnauer, R. Csencsits and T. Rajh, "Fe_2O_3 Nanoparticle structures investigated by X-ray absorption near-edge structure, surface modification and model calculations", *J. Phys. Chem. B.*, vol. 106, pp. 8539-8546, 2002.

[5] R. Turcu, I. Peter, O. Pana, L. Giurgiu, N. Aldea, B. Barz, M.N. Grecu, A. Coldea, "Structural and magnetic properties of polypyrrole nanocomposites", *Mol. Cryst. Liq. Cryst.*, vol. 417, pp. 235-243, 2004.

[6] N. Aldea, R. Turcu, A. Nan, I. Craciunescu, O. Pana, X. Yaning, Zhonghua Wu, D. Bica, L. Vekas and F. Matei, "Investigation of nanostructured Fe_3O_4 polypyrrole core-shell composites by X-ray absorption spectroscopy and X-ray diffraction using synchrotron radiation", *J.Nanopart. Res.*, vol. 11, pp. 1429-1439, 2009.

[7] B. E. Warren, "X-Ray Diffraction", Ed. New York: Dover Publication, 1969
[8] D. Balzar, "X Ray Diffraction Line Broadening: Modelling and Applications to High –Tc Superconductors", *J. Res. Nat. Inst. Stand. Technol.*, vol. 98, pp. 321-353, 1993.
[9] N. Aldea and E. Indrea, "XRLINE, a program to evaluate the crystallite size of supported metal catalysts by single x-ray profile Fourier analysis", *Comput. Phys. Commun.*, vol. 60, pp. 155-163, 1990.
[10] P. Marginean and A. Olariu, "Metal / Oxide support effects in the H_2-H_2O deuterium exchange reaction catalyzed by nickel", *J. Catal.*, vol. 95, pp. 1-12, 1985.
[11] S. Galvano and G. Parravano, "Chemical reactivity of supported gold: IV. Reduction of NO by H_2", *J. Catal.*, vol. 55, pp. 178–190, 1978.
[12] A. Ueda and M. Haruta, " Reduction of nitrogen monoxide with propane over Au/Al_2O_3 mixed mechanically with Mn_2O_3", *Appl. Catal. B*, vol. 18, pp. 115-121, 1998.
[13] N. Aldea, A. Gluhoi, P. Marginean, C. Cosma and X. Yaning, "Extended X-ray absorption fine structure and X-ray diffraction studies on supported nickel catalysts", *Spectrochim. Acta B*, vol. 55, pp. 997-1008, 2000.
[14] R. Grisel, K. J. Weststrate, A. Gluhoi and B. E. Nieuwenhuys, "Catalysis by gold nanoparticles", *Gold Bulletin*, vol. 35, pp. 39-45, 2002.
[15] A. Gluhoi, "Fundamental studies focused on understanding of gold catalysts" PhD diss., Leiden University, 2005
[16] BSRF. Activity Report 1993. Beijing Electron Positron Collider National Laboratory. NL-SH-013.
[17] N. Aldea and E. Indrea, "Fourier analysis of EXAFS and XANES data - a self-contained Fortran program-package - the third version", *Comput. Phys. Commun.*, vol. 60, pp. 145-154.
[18] N. Aldea, R. Zapotinschi and C. Cosma, "Crystallite size determination for supported metal catalysts by single X-ray profile Fourier analysis", *Fresenius J. Anal. Chem.*, vol. 355, pp. 367-369, 1995.
[19] C. Bonnelle, "X-ray Spectroscopy" in *Physical Methods in Advanced Inorganic Chemistry*, H. A. O. Hill and P. Day, Ed. New York: Interscience, 1968.
[20] N. Aldea, A. Gluhoi, P. Marginean, C. Cosma, Y. Xie, T. Hu, Whongua Wu and Baozhong Dong, "Investigation of supported nickel catalysts by X-ray absorption spectrometry and X-ray diffraction using synchrotron radiation", *Spectrochim. Acta Part B.*, vol. 57, pp. 1453-1460, 2002.
[21] A. San-Miguel, "A program for fast classic or dispersive XAS data analysis in a PC", *Physica B.*, vol. 208&209, pp. 177-179, 1995.
[22] D. C. Koningsberger and B. C. Gates, "Nature of the metal-support interface in supported metal catalysts: results from X-ray absorption spectroscopy", *Catal. Lett.*, vol. 14, pp. 271-277, 1992.
[23] C. H. Lin, S. H. Hsu, M.Y. Lee and S. D. Lin, "Active morphology of Au/γ-Al_2O_3-a model by EXAFS", *J. Catal.*, vol. 209, pp. 62-68, 2002.
[24] R. Zanella, S. Giorgio, C. H. Shin, C. R. Henry, and C. Louis, "Characterization and reactivity in CO oxidation of gold nanoparticles supported on TiO2 prepared by deposition-precipitation with NaOH and urea", *J. Catal.*, vol. 222, pp. 357-367, 2004.
[25] R. A. Young, R. J. Gerdes and A. J. C. Wilson, "Propagation of Some Systematic Errors in X-ray Line Profile Analysis", *Acta Cryst.*, vol. 22, pp. 155-162, 1967.
[26] J. S. Walker, "Fast Fourier Transform" 2nd ed., New York, London, Tokyo: CRC Boca Raton, pp. 104–112, 1997.
[27] F. Raiteri, A. Senin and G. Fagherazzi, "An automatic system for X –ray diffraction line profile analysis", *J. Mat. Sci*, vol. 13, pp.1717-1724, 1978.
[28] R. Turcu, Al. Darabont, A. Nan, N. Aldea, D. Macovei, D. Bica, L. Vekas, O. Pana, M.L. Soran, A.A. Koos and L. P. Biro, "New polypyrrole-multiwall carbon nanotubes hybrid materials", *J. Optoelectron. Adv. Mater.*, vol. 8, pp. 643-647, 2006.